

## Doping and Temperature Dependence of the Mass Enhancement Observed in the Cuprate $\text{Bi}_2\text{Sr}_2\text{CaCu}_2\text{O}_{8+\delta}$

P. D. Johnson,<sup>1</sup> T. Valla,<sup>1</sup> A. V. Fedorov,<sup>1,\*</sup> Z. Yusof,<sup>2</sup> B. O. Wells,<sup>2</sup> Q. Li,<sup>3</sup> A. R. Moodenbaugh,<sup>3</sup> G. D. Gu,<sup>4</sup> N. Koshizuka,<sup>5</sup> C. Kendziora,<sup>6</sup> Sha Jian,<sup>7</sup> and D. G. Hinks<sup>7</sup>

<sup>1</sup>*Department of Physics, Brookhaven National Laboratory, Upton, New York 11973-5000*

<sup>2</sup>*Department of Physics, University of Connecticut, 2152 Hillside Road U-46, Storrs, Connecticut 06269*

<sup>3</sup>*Division of Materials Sciences, Brookhaven National Laboratory, Upton, New York 11973*

<sup>4</sup>*School of Physics, University of New South Wales, P.O. Box 1, Kensington, New South Wales, Australia 2033*

<sup>5</sup>*Superconductivity Research Laboratory, ISTEC, 10-13, Shinonome I-chrome, Koto-ku, Tokyo 135, Japan*

<sup>6</sup>*Materials Sciences Division, Naval Research Laboratory, Washington, D.C. 20375*

<sup>7</sup>*Materials Sciences Division, Argonne National Laboratory, Argonne, Illinois 60439*

(Received 14 February 2001; published 8 October 2001)

High-resolution photoemission is used to study the electronic structure of the cuprate superconductor,  $\text{Bi}_2\text{Sr}_2\text{CaCu}_2\text{O}_{8+\delta}$ , as a function of hole doping and temperature. A kink observed in the band dispersion in the nodal line in the superconducting state is associated with coupling to a resonant mode observed in neutron scattering. From the measured real part of the self-energy it is possible to extract a coupling constant which is largest in the underdoped regime, then decreasing continuously into the overdoped regime.

DOI: 10.1103/PhysRevLett.87.177007

PACS numbers: 74.25.Jb, 74.72.Hs, 79.60.Bm

In any system, the electrons (or holes) may interact strongly with various excitations resulting in modifications to both their lifetime and binding energy. The quantity that describes these effects is the self-energy,  $\Sigma(\mathbf{k}, \omega)$ , the imaginary part representing the scattering rate or inverse lifetime, the real part, the shift in energy. An electron in a solid thus becomes “dressed” with a “cloud” of excitations, acquiring a different effective mass, but still behaving as a “single-particle” excitation or quasiparticle. This represents the traditional Fermi liquid picture. In more exotic materials, an electron or hole may lose its single-particle integrity and decay completely into collective excitations.

It has recently been demonstrated that angle-resolved photoemission (ARPES) is an excellent tool for momentum resolving self-energy effects. A measurement of  $\Sigma(\mathbf{k}, \omega)$  allows the determination of the coupling strength as well as the identification of the energy scale of the fluctuations involved in the coupling. Recently, self-energy effects due to the electron-phonon interaction have been identified in molybdenum [1] and beryllium [2], where the energy scale is represented by the Debye energy and in the layered dichalcogenide  $2\text{H-TaSe}_2$ , where the self-energy corrections reflect coupling to fluctuations in the charge density wave order parameter [3]. The extension of such studies to the realm of high- $T_C$  superconductivity allows the identification of the appropriate energy scales describing the fluctuations in these materials. However, it is not clear that a Fermi liquid methodology is appropriate for the high temperature superconductors. Indeed, a recent study of optimally doped  $\text{Bi}_2\text{Sr}_2\text{CaCu}_2\text{O}_{8+\delta}$  demonstrated the non-Fermi liquidlike nature of the material [4]. It was shown that the imaginary part of the self-energy follows a marginal Fermi liquid (MFL) behavior [5]. However, in the same study [4], a change in the mass enhancement was

observed in the superconducting state, indicating structure in the self-energy and the appearance of an energy scale well removed from the Fermi level. The corresponding change in  $\text{Im}\Sigma$  was not observed directly. Subsequent experimental studies have reported that in the superconducting state the mass enhancement exists over a large portion of the Fermi surface [6,7]. Theoretical studies have focused on the possibility that these observations reflect coupling to the magnetic resonance peak observed in inelastic neutron scattering (INS) studies [8].

In this Letter, we examine the doping and temperature dependence of the mass enhancement. We find that in the normal state the self-energy is well described within the framework of the MFL model. However, upon entering the superconducting state, changes occur in the ARPES spectra. We find that the self-energy correction and associated mass enhancement are strongly dependent on the hole doping level, decreasing continuously with doping. Further the energy scale observed in the superconducting state is linearly dependent on the transition temperature  $T_C$ . This dependence is almost identical to that observed for the resonant collective mode observed in INS studies [9,10].

The experimental studies reported here were carried out on a Scienta electron spectrometer with a momentum resolution of  $\sim 0.005 \text{ \AA}^{-1}$  and an energy resolution of  $\sim 10 \text{ meV}$  [11]. Photons were provided by a normal incidence monochromator based at the National Synchrotron Light Source. Samples of optimally doped ( $T_C = 91 \text{ K}$ )  $\text{Bi}_2\text{Sr}_2\text{CaCu}_2\text{O}_{8+\delta}$  were produced by the floating zone method [12]. The underdoping and overdoping was achieved by annealing optimally doped samples in argon [13] and in oxygen [14], respectively. All samples were mounted on a liquid He cryostat and cleaved *in situ* in

the UHV chamber with base pressure  $3 \times 10^{-9}$  Pa. The self-energy corrections were determined either from energy distribution curves (EDC) or from momentum distribution curves (MDC). The EDC represents the intensity as a function of binding energy at constant momentum and the MDC represents the intensity as a function of momentum at constant binding energy.

In Fig. 1 we show the photoemission intensities recorded as a function of binding energy and momentum in the  $(0,0)$  to  $(\pi, \pi)$  direction of the Brillouin zone for from left to right, the underdoped (UD), optimally doped (OP), and overdoped (OD)  $\text{Bi}_2\text{Sr}_2\text{CaCu}_2\text{O}_{8+\delta}$  samples, all in the superconducting state. In the lower panel we show the corresponding dispersions obtained from MDC's for the superconducting and normal states. It is clear that even in the normal state, the dispersion in the vicinity of the Fermi level deviates from the linear dispersion predicted by band structure calculations [15]. In the superconducting state, an additional modification to the dispersion develops for the UD and OP samples, while in the OD material there is no detectable change.

The spectra in Fig. 1 display other interesting features. For  $\omega \geq 50$  meV the velocity decreases with doping. Second, the spectral response is less well defined in the underdoped regime with the spectral width in both energy and momentum exceeding the amount of dispersion from  $k = k_F$ . Following recent suggestions of Orgad *et al.* [16] these two observations may be evidence of increased electron (hole) fractionalization in the underdoped regime.

In Fig. 2 we show the deviation,  $\text{Re}\Sigma$ , from the non-interacting dispersion as a function of binding energy for

both the superconducting and normal states. We define the noninteracting dispersion as a straight line that coincides with the measured Fermi point and the dispersion measured at a higher binding energy, typically 250 meV (see Fig. 1) where  $\text{Re}\Sigma$  is set to zero. The overall magnitude of the self-energy continuously decreases with doping in both the normal and superconducting states. We also show the difference in  $\text{Re}\Sigma$  between the superconducting and the normal state. We suggest that this difference represents *a change in the excitation spectrum* associated with the coupling upon entering the superconducting state. This change should also be manifested in measurements of  $\text{Im}\Sigma$ . While apparent in the underdoped regime [17], the effect is too subtle to observe directly in the optimally doped material.

In Fig. 3 we plot different quantities deduced from  $\text{Re}\Sigma$  as a function of the deviation from the maximum  $T_C = 91$  K, characterizing the optimally doped material. We plot both  $\omega_0$ , the energy of the maximum in  $\text{Re}\Sigma$  in the superconducting state, and  $\omega_0^{SC}$ , the energy of the maximum in the difference between the superconducting and the normal state. Since in the overdoped regime the difference between the superconducting- and normal-state dispersion vanishes, the energy scale characterizing the superconducting state could not be detected in the nodal region [18]. The characteristic energy was therefore identified for a limited range of overdoping and only by moving away from the node towards the  $(\pi, 0)$  region where the coupling is observed to be stronger while the characteristic energy of the kink remains momentum independent [7,19]. Indeed, measurements of the renormalized velocity in the

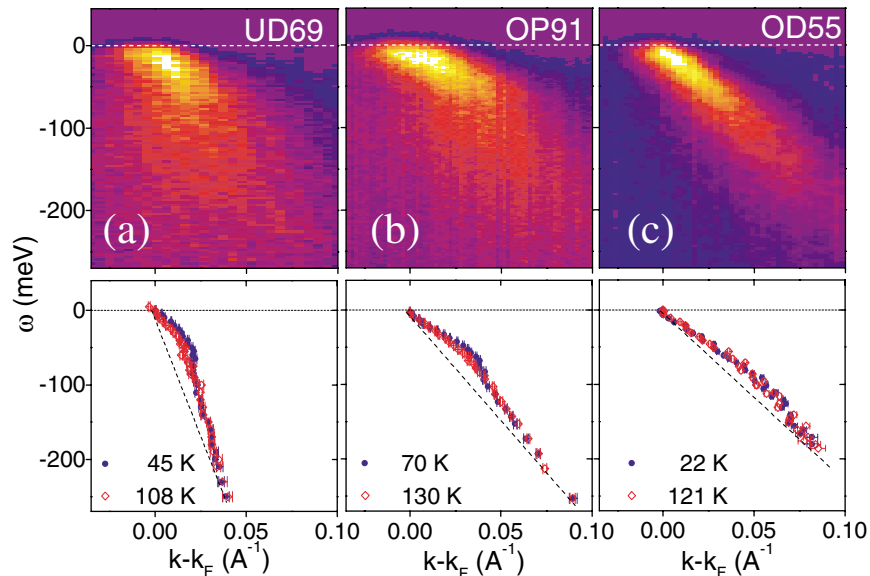


FIG. 1 (color). Upper panels: two dimensional photoemission intensities observed from (a) underdoped (UD), (b) optimally doped (OP), and (c) overdoped (OD) samples. The superconducting transition temperatures are indicated. Lower panels: the dotted lines indicate the MDC deduced dispersions for both the superconducting (blue dots) and normal states (open red diamonds) corresponding to the different samples in the panels above.

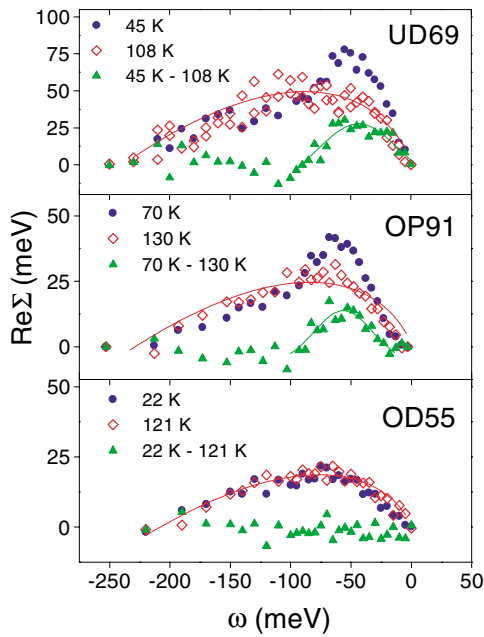


FIG. 2 (color).  $\text{Re}\Sigma$  as a function of binding energy for the superconducting (blue dots) and normal states (open red diamonds) for the UD69, OP91, and OD55 samples. The solid lines through the normal state data represent MFL fits to the data. The difference between the superconducting and the normal  $\text{Re}\Sigma$  for each level of doping is also plotted (green triangles). The lines through the latter are Gaussian fits to extract the peak energy  $\omega_0^{sc}$ .

superconducting state indicate that, for optimal doping, the coupling increases by a factor of 3 or more on moving towards the  $(\pi, 0)$  region [19].

It is clear that the characteristic energies scale linearly with  $T_C$  as opposed to the magnitude of the maximal gap which increases continuously on going into the underdoped regime [20]. When fitted with a straight line, the data points for  $\omega_0^{sc}$  and  $\omega_0$  in Fig. 3 yield  $\omega \sim 6k_B T_C$ .

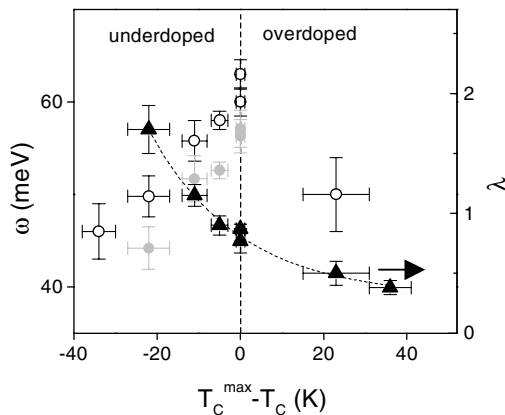


FIG. 3. Plot of  $\omega_0$ , the energy of the maximum value of  $\text{Re}\Sigma$  in the superconducting state (open circles), and  $\omega_0^{sc}$  (gray circles), the energy of the maximum in difference between the superconducting and normal state values plotted as a function of  $T_C$  referenced to the maximum  $T_C^{\max}$  ( $\sim 91$  K). The coupling constant  $\lambda$  (black triangles) is referenced to the right-hand scale.

This behavior is reminiscent of that reported in INS studies where all of the characteristic low-energy features in the superconducting state appear to scale with  $T_C$ . In particular, the resonance energy was found to scale as  $E_r \sim 5.4k_B T_C$  [10], while the spin gap scales as  $\Delta_s \sim 3.8k_B T_C$  [21]. The possibility that the kink reflects coupling to zone boundary longitudinal optical phonons has also been discussed [22]. However, recent neutron studies indicate that these phonons occur at the same energy, independent of doping or temperature [23]. This is in complete contrast to the doping dependence of the kink energy observed in the present study.

The real part of the self-energy may also be used to extract the coupling strength to the excitations involved in the coupling [24] via  $\lambda = -(\partial \text{Re}\Sigma / \partial \omega)_{E_F}$ , neglecting the momentum dependence of  $\Sigma$  in the narrow interval around  $k_F$ . The coupling constant  $\lambda$  shown in Fig. 3 for different samples in the superconducting state is obtained by fitting the low-energy part of  $\text{Re}\Sigma(\omega)$  to a straight line. We see that the coupling decreases continuously with increasing doping level.

Shown in Fig. 4, the “kink” and the magnetic resonance mode also display the same temperature dependence. Here the temperature dependence of  $\text{Re}\Sigma$  for the underdoped (UD69K) sample, measured at the characteristic energy  $\omega = \omega_0^{sc}$ , is compared with the intensity of the resonance mode measured in INS from an  $\text{YBa}_2\text{Cu}_3\text{O}_{6+x}$  sample with similar  $T_C$  [9]. The identical temperature dependence in Fig. 4 points to a common origin for both phenomena. Note that both features exist at temperatures significantly higher than  $T_C$ . The temperature range over which they lose intensity at the fastest rate appears close to  $T_C$ . However, they show finite intensity up to temperatures close to  $T^*$ , the pseudogap temperature. A recent INS study combined with ARPES on the same underdoped  $\text{Bi}_2\text{Sr}_2\text{CaCu}_2\text{O}_{8+\delta}$  sample ( $T_C = 70$  K) has reported similar results [25].

We have provided strong evidence that in the superconducting state the low-energy excitations are affected by the low-energy part of the spin fluctuation spectrum. The question naturally arises as to what is responsible for the mass

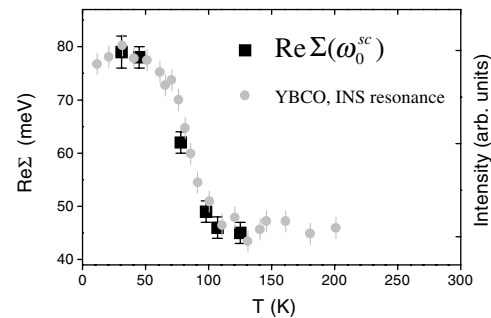


FIG. 4. Temperature dependence of  $\text{Re}\Sigma(\omega_0^{sc})$  from the nodal line for the UD69K sample (black squares) compared with the temperature dependence of the intensity of the resonance mode observed in INS studies of underdoped  $\text{YBa}_2\text{Cu}_3\text{O}_{6+x}$ ,  $T_C = 74$  K (Ref. [9]) (gray circles).

enhancement observed in the normal state for all samples. If phonons were the source of coupling, the scattering rate would saturate at frequencies greater than the highest phonon frequency ( $\leq 100$  meV) with a marked temperature dependence in that range [1,2,24]. This is clearly in contrast with optical conductivity [26] and photoemission [4,6,7] experiments, where the lack of saturation in the scattering rate points to the absence of a well-defined cutoff. More likely is the possibility that the enhancement still reflects coupling to spin excitations and that the spectrum of excitations changes with temperature. Indeed, the low-energy spin response change between the normal and the (pseudo)gapped state seems to be in one-to-one correlation with the changes in the low-energy part of the single-particle spectrum. The spin susceptibility has been shown to increase in the underdoped region in both the normal and superconducting states [27], consistent with the present findings. Further, as a two-particle response function, it is limited only by the bandwidth.

Any system with a scattering rate linear in binding energy should also display a logarithmic correction to the dispersion. Fitting the normal state  $\text{Re}\Sigma$  with the expression  $\text{Re}\Sigma = g'\omega \ln(\omega_c/\omega)$  (Fig. 2) gives a value of approximately 230 meV for  $\omega_c$  and values for  $g'$  consistent with the  $\omega$  dependence of  $\text{Im}\Sigma$  found in our earlier study [4] and with values obtained in a recent analysis of normal state EDC's [28].

To conclude, the doping, temperature, and momentum dependences of the various characteristic features seen in the cuprate photoemission spectra are consistent with a picture where the injected hole couples to the spin fluctuations observed in INS. Indeed, this evidence showing that the mass enhancement associated with the opening of the (pseudo)gap is electronic in nature is reminiscent of the behavior reported for 2H-TaSe<sub>2</sub> [3]. From the observation that in the underdoped region the transition temperature  $T_C$  decreases as the coupling increases, we conclude that the coupling strength alone is clearly insufficient to explain the superconductivity in these materials and that some other ingredients, such as the carrier concentration [17,29] and the phase coherence [30,31], are clearly required.

The authors acknowledge useful discussions with Alexei Tsvetlik, Andy Millis, V.N. Muthukumar, Dimitri Basov, Andrey Chubukov, John Tranquada, Steve Kivelson, and Takeshi Egami. The work was supported in part by the Department of Energy under Contract No. DE-AC02-98CH10886 and in part by the New Energy and Industrial Technology Development Organization.

---

\*Present address: Department of Physics, University of Colorado, Boulder, CO 80309-0390 and Advanced Light Source, Lawrence Berkeley National Laboratory, Berkeley, CA 94720.

- [1] T. Valla, A. V. Fedorov, P.D. Johnson, and S.L. Hulbert, *Phys. Rev. Lett.* **83**, 2085 (1999).
- [2] M. Hengsberger *et al.*, *Phys. Rev. Lett.* **83**, 592 (1999); S. LaShell, E. Jensen, and T. Balasubramanian, *Phys. Rev. B* **61**, 2371 (2000).
- [3] T. Valla *et al.*, *Phys. Rev. Lett.* **85**, 4759 (2000).
- [4] T. Valla *et al.*, *Science* **285**, 2110 (1999).
- [5] C. M. Varma *et al.*, *Phys. Rev. Lett.* **63**, 1996 (1989).
- [6] P. V. Bogdanov *et al.*, *Phys. Rev. Lett.* **85**, 2581 (2000).
- [7] A. Kaminski *et al.*, *Phys. Rev. Lett.* **86**, 1070 (2001).
- [8] M. Eschrig and M.R. Norman, *Phys. Rev. Lett.* **85**, 3261 (2000).
- [9] P. Dai *et al.*, *Science* **284**, 1344 (1999).
- [10] H. F. Fong *et al.*, *Nature (London)* **398**, 588 (1999); H. He *et al.*, *Phys. Rev. Lett.* **86**, 1610 (2001).
- [11] P.D. Johnson *et al.*, in *Synchrotron Radiation Instrumentation SRI 99*, edited by P. Pianetta, J. Arthur, and S. Brennan, AIP Conf. Proc. No. 521 (AIP, New York, 2000), p. 73.
- [12] G.D. Gu, K. Takamaku, N. Koshizuka, and S. Tanaka, *J. Cryst. Growth* **130**, 325 (1990); N. Miyakama *et al.*, *Phys. Rev. Lett.* **80**, 157 (1998).
- [13] A. R. Moodenbaugh, D. A. Fisher, Y.L. Wang, and Y. Fukumoto, *Physica (Amsterdam)* **268C**, 107 (1996).
- [14] C. Kendziora, R. J. Kelley, E. Skelton, and M. Onellion, *Physica (Amsterdam)* **257C**, 74 (1996).
- [15] H. Krakauer and W.E. Pickett, *Phys. Rev. Lett.* **60**, 1665 (1988).
- [16] D. Orgad *et al.*, cond-mat/0005457.
- [17] T. Valla *et al.* (to be published).
- [18] In the overdoped regime, there is more uncertainty in the transition temperature due to the increased tendency to lose oxygen. To minimize this,  $T_C$  was measured by monitoring the superconducting gap and by measuring the susceptibility before and after the photoemission.
- [19] T. Valla *et al.*, *Phys. Rev. Lett.* **85**, 828 (2000).
- [20] J. C. Campuzano *et al.*, *Phys. Rev. Lett.* **83**, 3709 (1999).
- [21] P. Dai, H. A. Mook, R.D. Hunt, and F. Doğan, *Phys. Rev. B* **63**, 054525 (2001).
- [22] A. Lanzara *et al.*, cond-mat/0102227; Z.-X. Shen, A. Lanzara, and N. Nagaosa, cond-mat/0102244.
- [23] Y. Petrov *et al.*, cond-mat/0003414; R. J. McQueeney *et al.*, cond-mat/0105593.
- [24] G.D. Mahan, *Many Particle Physics* (Plenum Press, New York, 1991).
- [25] J. Mesot *et al.*, cond-mat/0102339.
- [26] A. V. Puchkov, D. N. Basov, and T. Timusk, *J. Phys. Condens. Matter* **8**, 10049 (1996).
- [27] P. Bourges, in *The Gap Symmetry and Fluctuations in High Temperature Superconductors*, edited by J. Bok, G. Deutscher, D. Pavuna, and S. A. Wolf (Plenum Press, New York, 1998).
- [28] E. Abrahams and C. Varma, *Proc. Natl. Acad. Sci. U.S.A.* **97**, 5714 (2000).
- [29] H. Ding *et al.*, cond-mat/0006143.
- [30] V. J. Emery and S. A. Kivelson, *Nature (London)* **374**, 434 (1995).
- [31] I. Vobornik *et al.*, *Phys. Rev. Lett.* **82**, 3128 (1999); *Phys. Rev. B* **61**, 11 248 (2000).